Modified Agrawal Field-to-Transmission Line Method Based on Equivalent Total Tangential Electric Field Source Terms

Jean-Philippe Parmantier, Christophe Guiffault, Didier Roissé, Christophe Girard, Fabien Terrade, Solange Bertuol, Isabelle Junqua, Alain Reineix

Modified Agrawal Field-to-Transmission Line Method Based on Equivalent Total Tangential Electric Field Source Terms

Jean-Philippe Parmantier, Christophe Guiffaut, Didier Roissé, Christophe Girard, Fabien Terrade, Solange Bertuol, Isabelle Junqua, Alain Reineix

***Abstract*— This paper presents an application of a modified field-to-transmission-line-model inspired from Agrawal's model. In this model the field applied as a source term includes the tangential incident electric field as well as surrounding tangential scattered electric fields due to the current induced on the transmission-line. This weak domain decomposition approach allows one to calculate currents accounting for the reaction of those currents on the EM incident fields. The theoretical development is made on the basis of a two-wire transmission line; it is then extended to any transmission-line geometry. A numerical validation is made on several configurations of excitations of single wire transmission line networks. Particularly the results show that this model is able to predict the EM radiation of the cable. The paper concludes on future possible applications of this modified field-to-transmission-line approach in real applications of cable bundles in 3D structures of industrial complexity.**

***Index Terms*— Transmission-lines, Multiconductor, Thin wire model, Field-to-Transmission-Line, Cable bundles, Cable networks**

I. Introduction

Field-to-Transmission-Line (FTL) [1] is a well-known approach to model cables in 3D structures. The main interest of this model is to be easily extended to Multiconductor Transmission Line Network (MTLN) models [2] and to make possible MTLN calculations separately from 3D calculations. Nowadays, in the related numerical modelling process, the incident EM fields are collected on the routes of cable bundles (but in the absence of the bundles in the 3D model) and are then introduced as source terms for the MTLN model. The calculation time for the MTLN models is significantly smaller compared to the 3D full-wave calculation for determining the MTLN incident field source terms. Several formulations of FTL exist but Agrawal's formulation [3] based on incident electric tangential fields is the most appropriate for 3D numerical applications. The main interest of Agrawal's model is that the source terms are tangent to the cable routes which avoids the constraint of having to define transverse field components like in the two other FTL models, Taylor [4] and Rachidi [5]. This approach has been the subject of several applications of EM-coupling-on bundles in 3D structures ([6], [7], [8]). It is now well generalized in laboratories and industry for system-level modelling and has been successfully demonstrated on many complex wiring configurations ([6], [7], [8]). This approach is suitable for cable bundle design and installation, to optimize parameters such as cable types, cable shields, segregation distances, etc… This is particularly true in the perspective of the certification regulation on wiring installation [9].

Nevertheless, one of the main limitations of the FTL model is that it does not take into account the reaction of the currents induced by transmission-lines (TLs) onto the incident EM fields. EM coupling thereby results of incident fields only but coupling with scattered fields is not made. Several TL models have been proposed to overcome this limitation ([10], [11]) but their implementation for real complex cable bundle configurations in 3D structures does not seem yet to be as operatory as regular FTL models.

Of course such a current reaction can be obtained with meshed models of multiconductor wires or MTL models embedded in 3D full-wave models [12] but again those models are not mature enough to offer the same level of flexibility as FTL for system level modelling. Besides wire models currently applied in 3D models are generally limited to single thin wire models [13] or their derived-oblique models [14]-[16]. The idea of this paper is therefore to investigate how both MTL and thin-wire 3D-modeling approaches can be combined in order to solve this current-on-scattered EM-field reaction issue.

Section II of this paper establishes an analogy between a usual TL model made of two wires illuminated by an incident EM field and the thin wire model as currently used in 3D modelling; the modified FTL model is then obtained. In Section III, numerical verifications of the modified MTL model are made on several configurations of single-wire networks for both EM field illumination and lumped voltage source application. Finally Section IV concludes on the relevance of the modified FTL model for future applications on complex and realistic cable-bundle configurations.

This work was supported by the Direction Générale de l'Armement (D.G.A.), France.

J-P. Parmantier, S. Bertuol and I. Junqua are with ONERA, the French Aerospace Lab, Toulouse, France (email: jean-philippe.parmantier@onera fr)

C. Guiffaut and A. Reineix are with the XLIM Institute, University of Limoges and with le Centre National de la Recherche Française (C.N.R.S.), (e-mail: christophe.guiffaut@xlim.fr; alain.reineix@xlim.fr).

C. Girard and D. Roissé are with AxesSim, Strasbourg, France (email: christophe.girard@axessim.fr)

F. Terrade is with Dassault Aviation, Saint-Cloud, France (email: Fabien.Terrade@dassault-aviation.com)

II. Analogy between transmission-line and Holland's thin wire formalisms

A. Problem to solve

Our theoretical development starts from a reminder of the demonstration of the first TL equation applied on the same two-wire transmission line geometry as in [1]. We call the two parallel wires of the TL, "*signal wire*" and "*return wire*", each of them having a length ℓ and radiuses a_s and a_r respectively (Fig. 1). The distance between the two wires is *d*. In this paper, we do not make any restriction on a_s and a_r with respect to *d* since we do not explicitly need to calculate the per unit length (p.u.l.) inductance and capacitance parameters of the TL. The signal wire has a p.u.l. resistance R_{signal} and the return wire has a resistance p.u.l. R_{return}. *x* represents the longitudinal direction of the wires, *y* represents their transverse direction and *z* represents the direction normal to *x* and *y* passing by the two wires. The electrical current in the wires, *I(x)*, is in the *x* direction and is supposed to be uniformly distributed around the cross-section of the two wires. $V_{TL}^{tot}(x)$ is the voltage between the wires. We will see later in this paper that the "*tot*" subscript accounts for the total electromagnetic fields. The objective of the problem is to calculate *I(x)* on the signal wire.

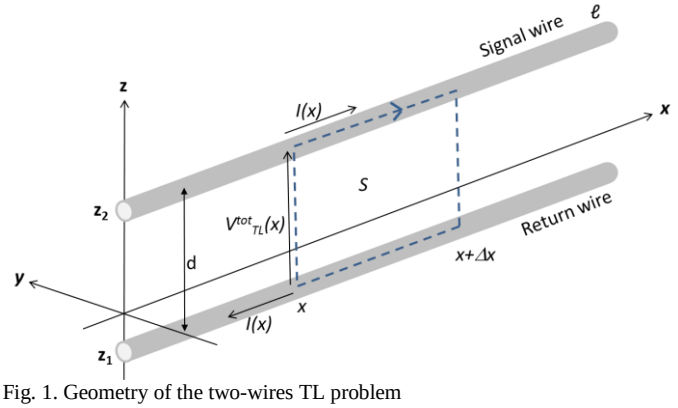

Fig. 1. Geometry of the two-wires TL problem

B. Notations for the application of the Faraday law

The theoretical developments presented in this paper all start from the Faraday Law on an open surface *S*. In homogeneous free space medium, we have in the frequency domain:

$$\iint_S rot\vec{E}\cdot ds = \oint_C \vec{E}\cdot dl = -j\omega\mu_0 \iint_S \vec{H}\cdot dS\,, \tag{1}$$

where *S* is the open surface bounded by a contour *C*.

We classically decompose the total EM fields $\{E^{tot}, H^{tot}\}$ as the sum of the incident EM fields $\{E^{inc}, H^{inc}\}$ (fields in the absence of the signal wire but in the presence of the return wire) and the EM scattered fields $\{E^{sca}, H^{sca}\}$ (fields due to the induced currents on the signal wire). We can thereby respectively write the electric and magnetic fields as:

$$\begin{aligned} E^{tot} &= E^{inc} + E^{sca} \\ H^{tot} &= H^{inc} + H^{sca} \end{aligned} \tag{2}$$

The EM field notations will be generalized as $E_\lambda^\alpha(x,y)$ and $H_\lambda^\alpha(x,y)$ for the electric and magnetic fields respectively, in which the subscript α stands either for "*tot*", "*sca*" or "*inc*" and λ for either *x*, *y* or *z*. In Fig. 1's geometry we remind the incident problem includes the return wire. In the following, we choose the integration surface *S* with a rectangular contour along the *x* axis, between *x* and x+Δx, and the z axis, between positions z_1 and z_2 (Fig. 2). Then, the limit $\Delta x \to 0$ is considered.

With those conditions, the Faraday law in (2) applies either on total, incident or scattered EM fields writes as:

$$\lim_{\Delta x\to 0}\left(j\omega\mu_0 \frac{\int_x^{x+\Delta x}\left(\int_{z_1}^{z_2}\left(H_y^\alpha(x,z)\right)\cdot dz\right).dx}{\Delta x}\right) = -\frac{dV_{z_1,z_2}^{\alpha}}{dx} - E_x^\alpha(x,z_2) + E_x^\alpha(x,z_1) \tag{3}$$

In which we define an equivalent voltage by:

$$V_{z_1,z_2}^{\alpha}(x) = -\int_{z_1}^{z_2} E_z^\alpha(x,z)\cdot dz \tag{4}$$

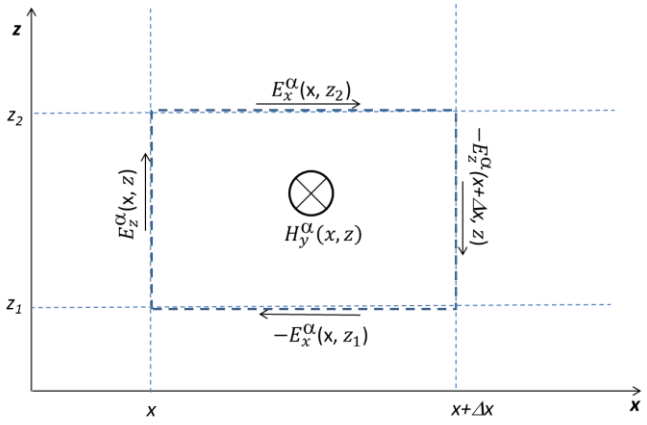

Fig. 2. Surface contour of integration in the x, z plane for the application of the Faraday law

C. Formulation of the TL equations

The application of (3) for the total fields gives the first TL equation based on Taylor's model [1]. According to Fig. 2 we take $z_1 = 0$ and $z_2 = d$. The voltage to be considered is the total voltage and the source term is expressed in terms of the incident transverse magnetic field in *S*:

$$\left(R_{TL} + j\omega L_{TL}\right)I(x) + \frac{dV_{TL}^{tot}(x)}{dx} = -\lim_{\Delta x\to 0}\left(j\omega\mu_0 \frac{\int_x^{x+\Delta x}\left(\int_0^{d}\left(H_y^{inc}(x,z)\right)\cdot dz\right).dx}{\Delta x}\right) \tag{5}$$

where

$$L_{TL}\cdot I(x) = \lim_{\Delta x\to 0}\int_x^{x+\Delta x}\left(\int_0^{d}\left(H_y^{sca}(x,z)\right)\cdot dz\right).dx \tag{6}$$

and R_{TL} represents the p.u.l. resistance of the transmission line, classically equal to the sum of the p.u.l. resistances of the signal wire and the return wire. We have:

$$R_{TL} = R_{signal} + R_{return} \tag{7}$$

where

$$R_{signal}I(x) = E_x^{tot}(x,d), \tag{8}$$

$$R_{return}I(x) = -E_x^{tot}(x,0), \tag{9}$$

$$V_{TL}^{tot}(x) = -\int_0^d E_z^{tot}(x,z)\cdot dz\,. \tag{10}$$

The application of (3) for the incident fields gives:

$$\lim_{\Delta x\to 0}\left(j\omega\mu_0 \frac{\int_x^{x+\Delta x}\left(\int_0^d \left(H_y^{inc}(x,z)\right)\cdot dz\right).dx}{\Delta x}\right) = -\frac{dV_{TL}^{inc}(x)}{dx} - E_x^{inc}(x,d) + E_x^{inc}(x,0) \quad (11)$$

with

$$V_{TL}^{inc}(x) = -\int_0^d E_z^{inc}(x,z)\cdot dz\,. \quad (12)$$

The application of (3) for the scattered fields gives:

$$j\omega L_{TL} I(x) = -\frac{dV_{TL}^{sca}(x)}{dx} - E_x^{sca}(x,d) + E_x^{sca}(x,0), \quad (13)$$

with

$$V_{TL}^{sca}(x) = -\int_0^d E_z^{sca}(x,z)\cdot dz\,, \quad (14)$$

generally defined as the "*scattered voltage*" [1].

In (5) we can introduce the following property:

$$V_{TL}^{tot}(x) = V_{TL}^{inc}(x) + V_{TL}^{sca}(x). \quad (15)$$

Then combining (5) and (11), we find the well-known Agrawal-formulation for which we remind that the voltage to be considered is the scattered voltage and the source term is expressed in terms of tangential incident electric fields at the level of the signal and return wires:

$$(R_{TL} + j\omega L_{TL})I(x) + \frac{dV_{TL}^{sca}(x)}{dx} = E_x^{inc}(x,d) - E_x^{inc}(x,0) \quad (16)$$

The 2nd transmission line equation is obtained in a way entirely similar to the one presented in [1]. The introduction of the scattered voltage in the 2nd transmission line equation formulated according to Taylor's model provides an equation without any right hand-side. We have then:

$$(G_{TL} + j\omega C_{TL})V_{TL}^{sca}(x) + \frac{dI(x)}{dx} = 0 \quad (17)$$

where:

- G_{TL} is the TL p.u.l. conductance,
- C_{TL} is the TL p.u.l. capacitance

The demonstration will not be reported in this paper since the focus is on the 1st TL.

From an application point of view, it is important to remember that even if the Agrawal-formulation involves only a scattered voltage which has no real existence, the current *I(x)* remains the "real" electrical current and the real voltages (total voltage) at the ends can always be obtained by applying the Ohm-law as far as end impedance loads are known, which is the case for EM simulation applications.

D. Signal wire in fictitious enveloping return contour

We consider the same geometry as the one in Fig. 1 with the signal wire parallel to the return wire and a separation distance *d* between the wires. Now we as well consider a small fictitious cylinder with an arbitrary cross-section surface of contour *C*, extending in the *x* direction around the whole signal wire path (Fig. 3). Similarly to the way to generate a unified TL model of a shielded cable with respect to a common reference conductor [17], we define three different TLs. We call:

- "*Inner TL*", the TL made of the signal wire with respect to the cylinder.
- "*Outer TL*", the TL made by the cylinder with respect to the return wire.
- "*Reference TL*", the TL made by the signal wire with respect to the return wire (the TL defined in the previous paragraph).

The TL model of the Inner TL is of particular interest in real 3D geometrical configurations since it is independent from a reference taken on the 3D structure.

As for (16), we start the derivation from the application of Faraday's law in its infinitesimal formulation (3). For this we define 3 reference points: a point of origin O_s on the signal wire and a point O_r on the return wire, both of them at the position *x* and a point *M* taken on the contour *C* of the cylinder at the same *x* position of O_s; the $\overrightarrow{O_sM}$ and $\overrightarrow{O_rM}$ vectors are perpendicular to the *x* direction.

We then define a cylindrical coordinate system local to the signal wire with an origin in O_s. In this system the ρ coordinate defining the position of *M* on the contour *C* varies between 0 and d_ρ.

The line between point *M* taken at position *x* and point *M'* taken at position $x+\Delta x$ allows us to decompose the surface of integration in two plane surfaces: one inner surface, $S_{int}(M)$, and one outer surface, $S_{out}(M)$. The inner surface is defined by the *x* direction and the $\overrightarrow{e_\rho}$ direction passing through O_s and *M*. The outer surface is defined by the *x* direction and the $\overrightarrow{e_h}$ direction passing by O_s and *M*. The *h* coordinate with respect to $\overrightarrow{e_h}$ varies between 0 and d_h. $\overrightarrow{\rho_n}$ and $\overrightarrow{h_n}$ vectors define the normal vectors to $S_{int}(M)$ and $S_{out}(M)$ respectively (the reader will pay attention not to make confusion with $\overrightarrow{e_\rho}$ and $\overrightarrow{e_h}$ definitions).

The application of (3) is made on the total EM fields marching on the integration contours made by the two $S_{int}(M)$ and $S_{out}(M)$ surfaces. Similarly to the derivation of (16), we find:

$$\begin{aligned} &E_x^{tot}(x,z=d) - E_x^{tot}(x,z=0) + \\ &\lim_{\Delta x\to 0}\left(\frac{-\int_0^{d_h}\left(E_h^{sca}(x+\Delta x,h) - E_h^{sca}(x,h)\right)\cdot dh}{\Delta x} + \right. \\ &\left. \frac{+\int_0^{d_\rho}\left(E_\rho^{sca}(x+\Delta x,\rho) - E_\rho^{sca}(x,\rho)\right)\cdot d\rho}{\Delta x}\right) + \\ &\lim_{\Delta x\to 0} j\omega\mu_0\left(\frac{\int_x^{x+\Delta x}\left(\int_0^{d_h}\left(\vec{H}^{sca}(x,h)\cdot\vec{h}_n\right)\cdot dh\right)dx}{\Delta x} + \right. \\ &\left. \frac{\int_x^{x+\Delta x}\left(\int_0^{d_\rho}\left(\vec{H}^{sca}(x,\rho)\cdot\vec{p}_n\right)\cdot d\rho\right)dx}{\Delta x}\right) = E_x^{inc}(x,z=d) - E_x^{inc}(x,z=0) \end{aligned} \quad (18)$$

where two specific voltages terms can be defined:

$$\frac{dV_{out}^{sca}(x)}{dx} = \lim_{\Delta x\to 0}\frac{-\int_0^{d_h}\left(E_h^{sca}(x+\Delta x,h) - E_h^{sca}(x,h)\right)\cdot dh}{\Delta x}, \quad (19)$$

the p.u.l. variation of the scattered voltage in the outer TL.

$$\frac{dV_{\text{int}}^{sca}(x)}{dx} = \lim_{\Delta x\to 0}\frac{-\int_0^{d_\rho}\left(E_z^{sca}(x+\Delta x,\rho) - E_z^{sca}(x,\rho)\right)\cdot d\rho}{\Delta x} \quad (20)$$

the p.u.l. variation of the scattered voltage in the inner TL.

From (3), we have also:

$$\lim_{\Delta x\to 0} j\omega\mu_0 \frac{\int_x^{x+\Delta x}\left(\int_0^{d_h}\left(\vec{H}^{sca}(x,h)\cdot\vec{h}_n\right)\cdot dh\right)dx}{\Delta x} = -\frac{dV_{out}^{sca}(x)}{dx} - E_x^{sca}(x,h=d_h)+E_x^{sca}(x,0) \quad (21)$$

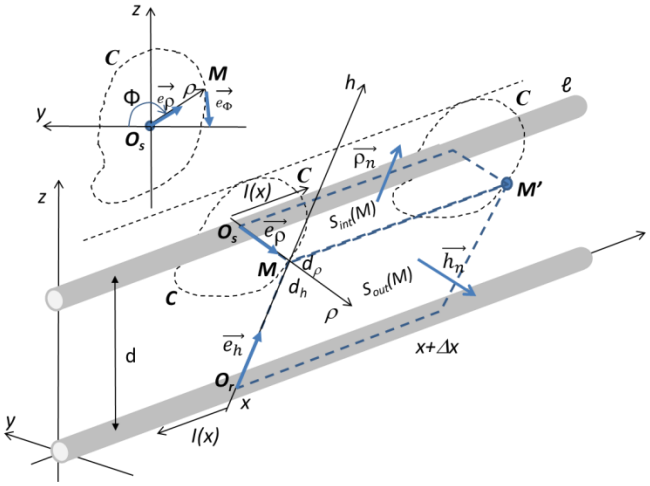

Fig. 3. The modified TL model made by the signal wire inside the fictitious cylinder together with its local cylindrical system

By introducing (21) in (18), we finally obtain:

$$R_{wire}I(x)+ j\omega\mu_0 \lim_{\Delta x\to 0}\frac{\int_x^{x+\Delta x}\left(\int_0^{d_\rho}\left(\vec{H}^{sca}(x,\rho)\cdot\vec{\rho}_n\right)\cdot d\rho\right)dx}{\Delta x} + \frac{dV_{\text{int}}^{sca}(x)}{dx} = E_x^{inc}(x,z=d)+E_x^{sca}(x,h=d_h) \quad (22)$$

Now the last step is to integrate (22) over the whole contour ***C***. For this, we introduce a curvilinear coordinate *u* allowing positioning point *M* anywhere over the contour. We note that:

$$\oint_C du = P \quad (23)$$

where *P* is the perimeter of *C*. A particular application is when the cylinder has a circular section of radius R_c. In this case, the *u* variable becomes: $du = R_c.d\Phi$ and $P = 2\pi R_c$.
We obtain:

$$\frac{\oint_C \frac{dV_{\text{int}}^{sca}(x)}{dx}\cdot du}{P} + R_{wire}I(x)+ j\omega\mu_0 \frac{\oint_C \frac{\lim_{\Delta x\to 0}\int_x^{x+\Delta x}\left(\int_0^{d_\rho}\left(\vec{H}^{sca}(x,\rho)\cdot\vec{\rho}_n\right)\cdot d\rho\right)dx}{\Delta x}\cdot du}{P} = E_x^{inc}(x,z=d)+\frac{\oint_C E_x^{sca}(x,h=d_h)\cdot du}{P} \quad (24)$$

In which we can introduce the definitions:

- The average scattered voltage in the inner TL defined by:

$$\left\langle V_{\text{int}}^{sca}(x)\right\rangle = \frac{\oint_C V_{\text{int}}^{sca}(x)\cdot du}{P} \quad (25)$$

- The p.u.l. inductance of the inner TL defined by:

$$L_{TL,\text{int}}I(x) = \mu_0 \frac{\oint_C \frac{\lim_{\Delta x\to 0}\int_x^{x+\Delta x}\left(\int_0^{d_\rho}\left(\vec{H}^{sca}(x,\rho)\cdot\vec{\rho}_n\right)\cdot d\rho\right)dx}{\Delta x}\cdot du}{P} \quad (26)$$

- The average scattered field on the *C* contour:

$$\left\langle E_x^{sca}(x)\right\rangle = \frac{\oint_C E_x^{sca}(x,h=d_h)\cdot du}{P} \quad (27)$$

In (24) we can also define an "*equivalent total tangential electric field*" at the level of the signal wire as the sum of the incident field at wire level and the average of the scattered tangent electric fields on the contour *C*:

$$\left\langle E_x^{tot}(x)\right\rangle = E_x^{inc}(x,z=d)+\left\langle E_x^{sca}(x)\right\rangle \quad (28)$$

With those definitions, we can now write (24), in the following compact form:

$$\left(R_{signal}+ j\omega\cdot L_{TL,\text{int}}\right)\cdot I(x)+\frac{d\left\langle V_{\text{int}}^{sca}(x)\right\rangle(x)}{dx} = \left\langle E_x^{tot}(x)\right\rangle \quad (29)$$

In (29), note that the equation does not depend anymore of the return conductor. Similarly to (17), the second TL equation writes:

$$j\omega\cdot C_{TL,\text{int}}\cdot\left\langle V_{\text{int}}^{sca}(x)\right\rangle(x)+\frac{dI(x)}{dx}=0 \quad (30)$$

where $C_{TL,int}$ is the p.u.l. capacitance of the inner TL.

This formalism can be applied to any types of full wave solvers together with their specific meshed geometrical models. (29) is obtained with a contour averaging for the sake of clarity of this paper but it can be recovered with an averaging over an area as well. The averaging process with many electric field component contributions increases accuracy as for oblique thin wire configurations for which the 2D symmetry observed for regular thin wires does not exist anymore and leads to non-uniform distribution of scattered electric field components around *C* [15].
In this paper we are particularly interested by the FDTD method when it is coupled with Holland's formalism [13] and its extensions for oblique thin wires [14]-[16]. In all cases for which regular thin-wire models are included along a Cartesian direction, the tangential fields along the wire result of an averaging of the electrical fields obtained by the FDTD method close to the wire. Note that each field component calculated by the FDTD method is an average field flux through a quad area. The average process leading to (29) applies even when the wire is located along a FDTD grid edge. Moreover, the total field quantity in (28) calculated by the FDTD method and located along the wire does not need to be zero as expected by the theory on a PEC wire because it must be understood as an average of fields around the wire.
Finally, the above whole theoretical development has been made with a two-wires TL as described in Fig. 1. However, as done in [1] for the derivations of Taylor's and Agrawal's FTL models, (29) and (30) can be extended to any geometrical configuration of the return conductor. In the following of this paper, the return wire will be replaced by a reference structure,

standing for example for a wire, a ground plane, a 3D surface etc...

E. Modified FTL formulation based on an equivalent "total" tangential electric field

We observe that (16) (for the reference TL) and (29) (for the inner TL) have TL equation forms. We have to remember that both equations are derived from an application of Faraday's law of the same problem. The difference in both equations is that the TL approximation (i.e. TEM mode) is required in the whole domain in (16) whereas it is required in the cylinder domain only in (29) which makes this formulation less restrictive and particularly adapted for 3D full-wave techniques with the possibility to update EM fields in the 3D model at the level of *C*.

Hereafter we want to make an analogy between the two equations in order to generalize (29) to a TL formulation of the reference TL as in (16). The objective is to overcome the usual FTL limitation consisting in not having the reaction of the current induced on the wires on the total field.

For this purpose we introduce the k_L coefficient defined as the ratio between the p.u.l. inductances of the reference TL and the inner TL respectively:

$$k_L = \frac{L_{TL}}{L_{TL,\text{int}}} \tag{31}$$

From (31) we derive the transformation of the p.u.l. capacitance:

$$C_{TL} = \frac{1}{v^2.L_{TL}} = \frac{1}{v^2.k_L L_{TL,\text{int}}} = \frac{C_{TL,\text{int}}}{k_L} \tag{32}$$

Then we multiply (29) by the k_L coefficient. We obtain:

$$\left(k_L R_{signal} + j\omega \cdot L_{TL}\right) \cdot I(x) + \frac{dV_{TL}^{eq}(x)}{dx} = k_L \left\langle E_x^{tot}(x) \right\rangle \tag{33}$$

If we introduce (32) in (30), we obtain:

$$j\omega \cdot C_{TL} \cdot V_{TL}^{eq}(x) + \frac{dI(x)}{dx} = 0 \tag{34}$$

In both (33) and (34) we introduce a new equivalent TL voltage definition:

$$V_{TL}^{eq}(x) = k_L \left\langle V_{\text{int}}^{sca}(x) \right\rangle (x) \tag{35}$$

In an analogous way as what is done in Agrawal's model in (16) and (17) which involve a scattered voltage, $V_{TL}^{sca}(x)$, the system of equations (33) and (34) involve an equivalent voltage definition, $V_{TL}^{eq}(x)$, which is not the real voltage. However both models provide the real current solution, *I(x)*. Besides, compared to (16) which uses the incident electric fields (namely $E_x^{inc}(x,d) - E_x^{inc}(x,0)$) as the right hand side term, (33) uses an analogous ($k_L \left\langle E_x^{tot}(x) \right\rangle$ term.

III. VALIDATION

A. Numerical methods used

In this section, the modified FTL method is validated on simple configurations of lossless one-wire networks over a PEC ground plane. As far as our validations are concerned the main advantage of these configurations is that we know that the wire networks will behave as antennas and that EM radiation of EM fields will be observed in a large frequency band which requires being able to model the reaction of EM fields scattered by induced currents.

All validation problems are solved with 3 methods:

- Method 1: with a full 3D calculation in which the wires under test are present. This calculation is considered to provide reference results.
- Method 2: with the classical Agrawal's FTL approach based on Agrawal's model in which the 3D calculation does not include the wire under test and provide incident electric fields along the route
- Method 3: with the modified FTL model developed in this paper in which the 3D calculation includes the wire under test and provide total electric fields along the route

All the field calculations in the 3 methods are performed with the TEMSI-FD solver developed by the XLIM Institute [18]. Fig. 4 represents the geometry of the problem as it is depicted by TEMSI-FD. The calculations of the MTLN responses in methods 2 and 3 are made using the CRIPTE code based on the resolution of the BLT equation in frequency domain [2] and developed by ONERA [19]. In both FTL methods (2 and 3), note that the field source terms must be applied on the horizontal wire as well as on the two vertical wires connecting the horizontal wires on the PEC ground planes.

B. One-wire validation test-case

1) Presentation of the test-case

The first geometrical configuration is made of a thin victim wire of radius 0.1 mm and length 2 m, called "victim wire", running in parallel in the *x* direction over a PEC and finite-dimensions ground plane (1.5 m x 1.5 m) at a 10-cm height (Fig. 4). Two vertical wires of similar radiuses connect it to the ground plane at which level two lumped resistances equal to 1 Ohm have been applied. On the lower side of the PEC plane, in the same *x*-*z* plane as the victim wire, another wire, called "excitation wire", with the same radius and height as the victim wire is running in the *x* direction; it is connected to two vertical wires as above the ground plane but this time with a resistive load of 50 Ω on the left hand side (low x-value end) and a short-circuit on the right hand side (large x-value end). In this geometry, a lumped voltage generator can be applied at the level of the ground plane on either the left-hand-side extremities of the victim wire or the excitation wire.

In the MTLN model of the victim wire, the model of the TL is approximated as a wire over an infinite ground plane and the vertical wires have the same p.u.l. electrical parameters as these of the horizontal line (usual conic antenna approximation [20]). The cell-size in the FDTD model has been chosen equal to 2 cm and Perfectly Matched Layers (PML) absorbing conditions surround the useful calculation-domain box of size 3.4 m x 3.4 m x 0.4 m. Time domain calculations have been made by applying on one of the two wires a lumped voltage generator with a Gaussian waveform of a frequency content up to 1 GHz. Then all currents induced on the victim wire and calculated either directly in Method 1 or by FTL and modified FTL approaches in Methods 2 and 3 (through tangential electric fields computed in the 3D simulation) have been Fourier transformed. All currents obtained by the 3 methods have been normalized to the Gaussian waveform.

The objective is to observe the current on the victim wire at two positions: at the left hand side extremity ("I_1") and in the middle ("I_{middle}"). The excitation wire is always included in the 3D model.

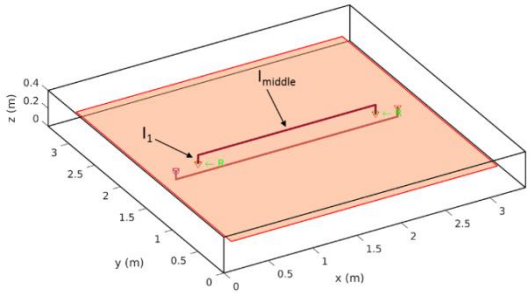

Fig. 4. Geometrical configuration used for the validation on a single TL The rectangular box indicates the position of the PML layers

2) Field illumination configuration

In this configuration, the lumped generator including the 50 Ω resistive load is applied on the left-hand-side extremity of the excitation wire at the level of the ground plane; the incident field applied on the victim wire is generated by the current developed on this excitation wire. The results of currents obtained at the two observation test points on the victim wire are presented in Fig. 5.

On the one hand, we observe that the classical Agrawal FTL method perfectly works from DC up to about 20 MHz, i.e. for quasi-static regime but not in the resonance regime of the wire. In the resonance regime, the FTL model does not capture properly the amplitude of the resonance peaks observed in the reference results, even if the resonance frequencies are well predicted.

On the other hand, the modified FTL entirely predicts the reference results on the whole frequency band. The comparison is almost perfect at the left hand side extremity (I_1) since the modified approach results fully overlap the reference calculated current. We do not observe such a perfect matching in the middle of the wire (*middle*) but we note that this discrepancy also appears in Agrawal's classical FTL. We attribute this discrepancy to the fact that the TL approximation does not perfectly work outside the extremities of the line certainly due to so-called "common antenna mode currents" as explained in [1].

3) Victim wire voltage excitation configuration

A lumped generator including a 1 Ω resistive load is now applied on the left-hand-side extremity of the victim wire at the level of the ground plane. This configuration is more challenging for our validation since no incident field is applied on the victim wire: especially the response of the victim wire can be directly obtained from a straightforward unique TL model exciting the victim wire with a 1V voltage generator. Nevertheless, we can also apply the modified FTL model and see the effect of the equivalent total field source terms (here equal only to the average scattered tangential electric field around the wire).

The conclusions are the same as for the former field illumination configuration; especially in this configuration the modified FTL approach allows taking into account the EM radiation of the wire. We even observe that the current at the center is better predicted than in the illumination configuration, certainly because a pure differential mode is excited on the TL and no common antenna mode currents is generated, which does not mean that this configuration does not radiate EM fields.

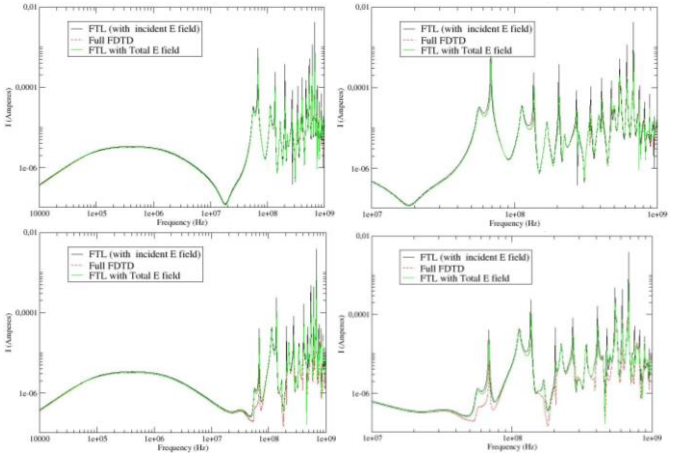

Fig. 5: Field illumination configuration (local voltage generator on the excitation wire) - Comparisons of currents obtained at the left-hand-side extremity (I_1, above) and in the center of the wire (*middle*, below) between full-3D (Method 1 – label "*Full FDTD*"), classical Agrawal's method (Method 2 – Label "*FTL (with incident E field)*") and modified FTL method (Method 3 – label "*FTL with Total E field*"). On the left hand side full frequency range. On the right hand side, high frequency range.

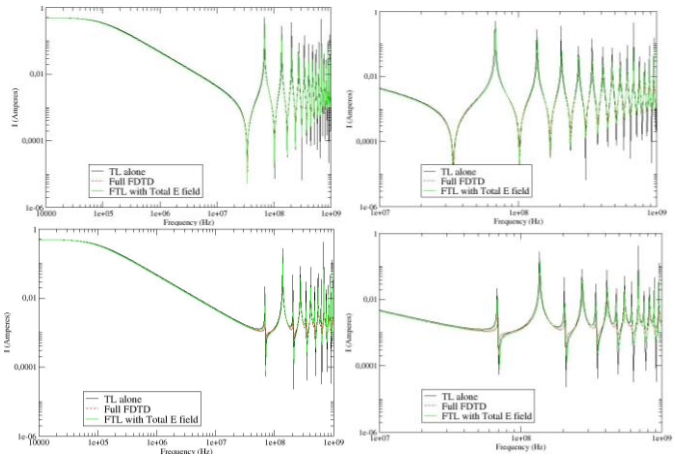

Fig. 6: Victim-wire voltage excitation configuration (local voltage generator on the victim wire) - Comparisons of currents obtained at the left-hand-side extremity (I_1, above) and in the center of the wire (*middle*, below), between full-3D (Method 1 – label "*Full FDTD*"), classical TL model (Method 2 – Label "*TL alone*") and modified FTL method (Method 3 – label "*FTL with Total E field*"). On the left hand side full frequency range. On the right hand side, high frequency range.

C. Branched network configuration

The previous test-case concerned only one TL but it is important to evaluate the robustness of the modified FTL model for branched network configurations, even if the previous single-TL test-case already included network aspects because of the connection of the two vertical wires to the horizontal wire. The PEC ground plane dimensions are 2.3 m x 1.7 m. Other main dimensions are reported in Fig. 7. A straight wire of radius 5 mm is connecting two metal boxes at the level of two connection points called "*connector A*" and

"*connector B*" and a transverse wire of radius 5 mm connects this straight wire to a connector C at the level of the ground plane with a vertical wire. As for the previous single TL test-case, an excitation wire is running under the ground-plane in the direction of the straight wire. All wires, including the excitation wire are at a 10 cm height above or below the PEC ground plane. The mesh size in the 3D-model is 2.5 cm. Note that the two metal boxes are meshed in the 3D model as well as the excitation wire.

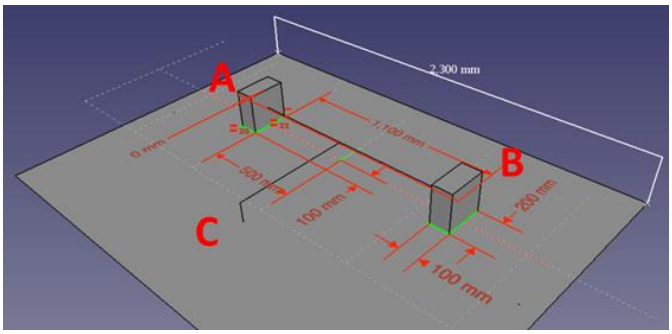

Fig. 7. Geometrical configuration used for the validation on branched networks

Fig. 8 presents the currents obtained at connector A in two loads configurations when all wire ends are either on 50 Ω or on short-circuits. Full 3D FDTD reference results match those obtained with the modified FTL model. Despite some signal processing issues observed at low frequencies, the same conclusions as for the single TL can be drawn. The modified FTL model allows us to reproduce the wire radiation losses in the resonance region. The small shift observed in the short-circuit configuration are not fully explained up to now but time to frequency signal processing is highly suspected due to time domain signals not fully returned to zero.

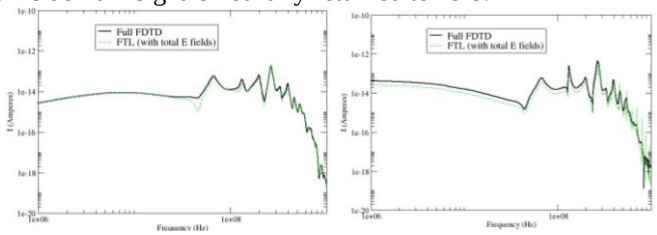

Fig. 8. Currents at end A on the branched network configuration when all extremities are loaded on 50 Ω (left) and short-circuit (right)

IV. Conclusion and Prospects

In this paper, we presented an extension of Agrawal's FTL model in a frequency domain formulation that includes the reaction of the induced current on the scattered field. The formulation is obtained by establishing the relationship between two TL models of an electrical wire in a 3D structure. The first TL is made by the wire inside a fictitious surrounding cylinder. The second TL is made by the wire with respect to the 3D structure: this model is directly derived from the first TL model by the multiplication with a k_L factor equal to the ratio of the p.u.l. inductances of the first and second TL models. We thereby obtain the modified FTL model, making the analogy with the usual Agrawal's model. As Agrawal's model, the MTLN model is referred to the 3D structure and can run independently from the 3D model. However there are some differences:

- The source term is defined as an equivalent total tangential field made of the usual incident tangential electric field to which a scattered tangential electric field on the surface of a surrounding cylinder is added. This source term is multiplied by the k_L factor.
- The p.u.l. resistance of the TL with respect to the 3D structure is also multiplied by the k_L factor.
- An equivalent voltage is defined along the TL. As for Agrawal's scattered voltage, this voltage is not used as such since its definition is quite complicated. Only the current is practically used in the resolution.

Validations have been made on single-wire TL networks over PEC ground planes for both EM field illumination and direct voltage generator application by computing EM source fields with a FDTD model. Results have been compared with full-3D calculations in which the single-wires were parts of the 3D mesh. In these applications with FDTD models, the modified FLT appears as a formulation in the frequency domain of the well-known Holland model (or its derivatives for oblique wires) in which the process of exchange and update of EM fields is now made a posteriori.

Despite its theoretical interest, we must admit that the use of this modified model in future applications is not straightforward. The objective of the modified FTL approach is indeed to have an approach similar to Agrawal's FTL model in which field terms are used as a distributed source terms applied in a MTLN model. Actually, the main interest of Agrawal's model (or Taylor's or Rachidi's model) is that the sources terms are based on incident fields, which means that they are calculated with a full-wave calculation in the absence of the cables and any type of multiconductor cable can be used since the same incident field terms can be applied on the wires (provided the wires have the same route as the route on which the incident field have been determined). In the modified FTL model, the wires have to be present in the full-wave calculation. So we can ask ourselves the following question: what is the interest of making another calculation with a TL model when the 3D calculation has already provided the solution of the currents on the wire?

As a matter of fact, the foreseen interest of this approach is clearly for MTLN applications. Indeed, as far as Multiconductor TL (MTLs) are concerned, we can anticipate that the scattered fields to be exchanged at the cylinder surface are dominated by the total current generated by all the wires of the MTL. This means that, provided an equivalent wire model of the MTL can be obtained, the scattered EM fields on the cylinder surface can be used and applied as source terms for each equivalent wire of the MTL, as done for usual FTL models. Several references have already investigated this problem of an equivalent wire or MTL models ([21], [22]) and could be used for this purpose.

Finally, the requirement to have to define a fictitious cylinder could be certainly bypassed applying techniques such as test-wires [23]. This technique allows the derivation of the source terms to be applied on a TL model thanks to the knowledge of the distribution of currents along the test-wire and the p.u.l. electrical parameters of its TL. From a practical point of view,

the test-wire is included in the 3D model and the currents along this wire are collected. Such a technique could be advantageously applied on our problem of the TL in the cylinder. Indeed the source terms obtained from the application of the test-wire method would be directly the ones derived in (28).

Another possibility could be to choose appropriately the geometry of the cylinder; namely, a circular cylinder making a coaxial TL would be the simplest choice allowing easy determination of the inner TL p.u.l. electrical parameters, and therefore of the k_L factor.

All these perspectives will be the subjects of future investigation for determining the scope of practical application of this formalism for real cable bundle configurations.

REFERENCES

[1] F.M. Tesche, M.V. Ianoz, T. Karlsson, "*EMC Analysis Methods and Computational Models*", John Wiley & Sons, pp.247-266. 1997.

[2] C. E. Baum, T. K. Liù, F. M. Tesche, "*On the Analysis of General Multiconductor Transmission-Line Networks, Interaction Notes*", Note 350, November 1978

[3] A.K. Agrawal, H.J. Price and S.H. Gurbaxani, "*Transient Response of Multiconductor-Transmission-Line Excited by a Non Uniform Electromagnetic Field*", IEEE Trans. EMC, 22, 1980, 119-129.

[4] C.D. Taylor, R.S. Satterwhite and C.H. Harrison, "*The Response of a Terminated Two-Wire Transmisison Excited by a Nonuniform Electromagnetic Field*", IEEE Trans. Antenna Propoag., 13, 1965, 987-989

[5] F Rachidi, "*Formulation of the field-to-transmission-line coupling equations in terms of magnetic excitation field*", IEEE Transactions on EMC, 1993

[6] L. Paletta, J-P. Parmantier, F. Issac, P. Dumas, J.-C. Alliot, ***"****Susceptibility analysis of wiring in a complex system combining a 3-D solver and a transmission-line network simulation"*, IEEE Trans. on EMC, Vol. 44, No. 2, May 2002, pp. 309-317.

[7] X. Ferrières, J-P. Parmantier, S. Bertuol, A. Ruddle, *"Application of Hybrid Finite Difference / Finite Volume to Solve an Automotive problem"*, IEEE Trans. on EMC, vol 46, n°4, pp. 624, 634, November 2004

[8] S. Arianos, M. A. Francavilla, M. Righero, F. Vipiana, P. Savi, S. Bertuol, M. Ridel, J-P Parmantier, L. Pisu, M. Bozzetti and G. Vecchi, *Evaluation of the Modeling of an EM Illumination on an Aircraft Cable Harness* , IEEE Trans. Electromagn. Compat. - Vol. 56, No. 4, August 2014

[9] FAA Advisory Circular "*Certification of Electrical Wiring Interconnection Systems on Transport Category Airplanes*", AC No. 25.1701-1

[10] H. Haase, J. Nitsch, T. Steinmetz, "*Transmission-Line Super Theory: a New Approach to an Effective Calculation of Electromagnetic Interactions*", Radio Sci. Bull. 307, pp. 33-60, 2003.

[11] F. Rachidi, S. Tkachenko: "*Electromagnetic Field Interaction with Transmission-lines*", Advances in Electrical Engineering and Electromagnetics #5, 2008

[12] J.-P. Berenger, "A multiwire formalism for the FDTD method," *IEEE Trans. Electromagn. Compat.*, vol. 42, no. 3, pp. 257–264, Aug. 2000.

[13] R. Holland and L. Simpson, "Finite-Difference Analysis of EMP Coupling to Thin Struts and Wires," *IEEE Trans. Electromagn. Compat.*, vol. 23, no. 2, pp. 88–97, May 1981.

[14] F. Edelvik, "A new technique for accurate and stable modeling of arbitrarily oriented thin wires in the FDTD method," *IEEE Trans. Electromagn. Compat.*, vol. 45, no. 2, pp. 416–423, May 2003.

[15] C. Guiffaut, A. Reineix and B. Pecqueux, "New oblique thin wire formalism in the FDTD method with multiwire junction," *IEEE Trans. Antennas and Propag*., vol. 60, no. 8, pp. 1458–1466, Marsh 2012.

[16] C. Guiffaut, N. Rouvrais, A. Reineix and B. Pecqueux, "Insulated oblique thin wire formalism in the FDTD method," *IEEE Trans. Electromagn. Compat.*, vol. 59, no. 5, pp. 1532–1440, October 2017.

[17] P. Degauque et J-P. Parmantier, "*Chapitre 2 : Couplage aux structures filaire" in "Compatibilté Electromagnétique*", Collection technique et scientifique des télécommunications. Lavoisier, Hermes.Paris 2007. under the direction of P. Degauque and A. Zeddam. In French

[18] *Time ElectroMagnetic Simulator – Finite Difference software*, TEMSI-FD, CNRS, Univ. of Limoges, Limoges, France, 2017 version.

[19] J. P. Parmantier, S. Bertuol, and I. Junqua, "*CRIPTE : Code de réseaux de lignes de transmission multiconducteur - User's guide – Version 5.1*" ONERA/DEMR/T-N119/10 - CRIPTE 5.1 2010.

[20] E. F. Vance, "Shielding Cables", Wiley 1978, ISBN 10: 0471041076

[21] C. Poudroux, M. Rifi, and B. Démoulin, "*A simplified approach to determine the amplitude of transient voltage on the cable bundle connected on non linear loads*," *IEEE Trans. Electromagn. Compat.*, vol. 37, no. 4, pp. 497–504, Nov. 1995.

[22] G. Andrieu, L. Koné, F. Bocquet, B. Démoulin, J-P. Parmantier, "*Multiconductor Reduction Technique for Modeling Common Mode Current on Cable Bundles at High Frequency for Automotive Applications*". IEEE Trans; on EM Compatibility, vol 50, n°1, February 2008

[23] J-P. Parmantier, I. Junqua, S. Bertuol, F. Issac, S. Guillet, S. Houhou, R. Perraud, "*Simplification Method for the Assessment of the EM Response of a Complex Cable Harness*" 20th International Zurich Symposium on EMC, 12-16 Jan. 2009

[24] J.P. Parmantier, "*The test-wiring method"*. Interaction Notes. Note 553. October 1998 (available at http://ece-research.unm.edu/summa/notes/)